Journal of Intelligent Systems and Internet of Things
Vol. 11, No. 02, PP. 97-110, 2024
DOI: https://doi.org/10.54216/JISIoT.110209

Enhanced Jaya Optimization Algorithm with Deep Learning Assisted Oral Cancer Diagnosis on IoT Healthcare Systems

R. Rajkumar[1], Dınesh Valluru[2], Siva Satya Sreedhar P. [3], N. Ramshankar[4], Sujatha S. [5], Somasundaram R.[6], M. Sudha[7], S. Navaneethan[8,*]

[1]Department of ECE, Vel Tech Rangarajan Dr. Saguthala R&D institute of Science and Technology, Chennai, Tamil Nadu, India
[2]Department of IT, MLRITM Engineering College, Hyderabad, India
[3]Department of Information Technology, Seshadri Rao Gudlavalleru Engineering College, Gudlavalleru, Krishna district, Andhra Pradesh, India
[4]Department of Computer Science and Engineering, R. M. D. Engineering College, Kavaraipettai, Tiruvallur, Tamil Nadu, India
[5]Department of Electronics and communication Engineering, Christ University, School of Engineering and Technology, Bangalore, India
[6]Management Studies Department, Kongu Engineering College, Erode 638060 India
[7] Department of ECE, Paavai Engineering College (Autonomous), Namakkal,Tamilnadu, India
[8]Department of ECE, Saveetha Engineering College, Chennai. Tamil Nadu, India
Emails: rajkumarramasami@gmail.com; dinesh.valluru15@mlritm.ac.in; sivasatyasreedhar@gmail.com; dr.ramshankar6@gmail.com; sujatha.s@christuniversity.in; rssundhar.mba@kongu.edu; gunasudhaa@gmail.com; navaneethans@saveetha.ac.in

Abstract

Recently, healthcare systems integrate the power of deep learning (DL) models with the connectivity and data processing capabilities of the Internet of Things (IoT) to enhance the early recognition and diagnosis of disease. Oral cancer diagnosis comprises the detection of cancerous or pre-cancerous abrasions in the oral cavity. Timely identification is essential for successful treatment and enhanced prognosis. Here is an overview of the key aspects of oral cancer diagnosis. One potential benefit of utilizing DL for oral cancer detection is that it analyses huge counts of data fast and accurately, and it could not need clear programming of the rules for recognizing abnormalities. This can create the procedure of detecting oral cancer more effective and efficient. Thus, the study presents an Enhanced Jaya Optimization Algorithm with Deep Learning Based Oral Cancer Classification (EJOADL-OCC) method. The presented EJOADL-OCC method aims to classify and detect the existence of oral cancer accurately and effectively. To accomplish this, the presented EJOADL-OCC method initially exploits median filtering for the noise elimination. Next, the feature vector generation process is performed by the residual network (ResNetv2) model with EJOA as a hyperparameter optimizer. For accurate classification of oral cancer, a continuously restricted Boltzmann machine with a deep belief network (CRBM-DBN) model. The simulated validation of the EJOADL-OCC algorithm is tested by the series of simulations and the outcome demonstrates its supremacy over present DL approaches.

Received: August 23, 2023, Revised: December 17, 2023 Accepted: January 29, 2024

Keywords: Healthcare; Oral cancer; Deep learning; Computer-assisted diagnoses; Internet of Things; Jaya Optimization Algorithm; Medical imaging

1. Introduction

Oral cancer is the major typical head and neck carcinoma and is now creating a worldwide concern and showing a better incidence rate [1]. It is a main cause of mortality and morbidity and hence, needs an early and quick identification for a good diagnosis. Initial-stage diagnosis is highly significant for better treatment, diagnosis, and survival [2]. Late prognosis has hindered the search for accurate remedy in spite of the current advancement in the understanding of molecular cancer mechanism [3]. Thus, the deep machine learning (ML) algorithm was touted to enrich early diagnosis, and subsequently diminish cancer-related demise. Automatic image evaluation support physicians and diagnosticians in the primary phase recognition of OSCC and in taking verdicts about cancer organization [4].

Presently, conventional oral examination (COE) comprising tactile and visual assessment (then tissue biopsy when it has some suspicious findings) was the routine process in the precursor disease and oral cancer management [5]. But, one disadvantage of COE is that numerous attributes of oral cancer can mimic aphthous ulcers and benign, and they were medically heterogeneous and subtle for dental surgeons to differentiate. Secondly, due to sampling bias and its invasive nature that can result in misdiagnosis or underdiagnosis, a biopsy will not often be considered a broadcasting tool. Additionally, although specialists can detect many features that distinguish cancerous lesions and benign the number of health resources and specialists is limited and focused on areas [6], affecting a big part of the oral tumor problem to fall on the community with lesser resources. Hence, an adjunctive help the current process gains popularity because of the ideology of accomplishing a low-cost screening method [7].

Among various methods, Artificial intelligence (AI) is typically used betwixt diverse regions of medicines. Sophisticated imaging technologies and Radiology, pathology, dermatology ophthalmology, were the disciplines to which it has made major contributions. In all cases, the count of obstacles should be evaluated [8]. Three components that were typically leveraged are generally utilized for applying the regulations: the amount of human involvement, the risk to safety of patients, and the occurrence of a prediction method. Machine learning (ML) was utilized used in oral cancer research for exploring the discretization among poorly oral squamous cell carcinoma (OSCC) or moderately differentiated and well-discriminated (WD) OSCC [9], for evaluating its capability to forecast disease outcomes, for forecasting the presence of lymph node metastasis of initial-step oral tongue squamous cell cancer. Currently, DL methods have shown a comparative benefit over feature-related region-related techniques in medical image analysis [10]. Various research works showed that DL methods can exceed the efficiency of human experts in several disease detection cases.

This study develops an Enhanced Jaya Optimizer Algorithm with DL-Based Oral Cancer Classification (EJOADL-OCC) method. The presented EJOADL-OCC technique initially exploits median filtering (MF) for noise elimination. Next, the feature vector generation process is performed by the residual network (ResNetv2) model with EJOA as a hyperparameter optimizer. For accurate classification of oral cancer, a continuously constrained Boltzmann machine with a deep belief network (CRBM-DBN) model is employed. The simulated analysis of EJOADL-OCC method is tested by the series of simulations.

2. Related Works

The authors in [11], intend to develop a novel DL approach termed D'OraCa to segment oral cancers employing clear imaging. The authors first developed a mouth diagnosis model for the oral image and incorporated it into the oral cancer classification technique as a guide for enriching the classifier performance. The authors assess the performance of 5 distinct MobileNetV2 and deep CNNs has opted as the feature extractors for this devised mouth landmark detection method. In [12], the authors explore the effective applications of DL and CV methodologies in the oral cancer region as regards clear images and inspected forecasts of automatic mechanisms to find oral malignant disorders with 2 stage pipeline. These preliminary outcomes validate the possibility of DL-related methods for the automatic classification and recognition of oral lesion in real-time.

Lu et al. [13] presented a fully automatic pipeline for detecting oral cancer on whole slide cytology imageries. The pipeline contains fully convolution regression-oriented nucleus recognition, next CNN-based classification, and per-cell focus selection. The authors [14] presented a DL method for an automatic, computer-assisted oral cancer detection mechanism by inspecting patient hyperspectral images (HSIs). For accurate medical image classification, the authors demonstrated an innovative structure of partitioned deep CNNs with 2 partitioned layers for label and classifying by labelling RoI in multi-dimensional HSIs. In [15], the authors have implemented and assessed the usefulness of 6 DCNN methods utilizing TL, to identify pre-tumorous tongue lesion through smaller data of medically annotated photographic images for diagnosing initial symptoms of OCC.

A new technique to compile bounding box annotations from many doctors is given in [16]. Following this, DNNs are utilized to construct automatic systems, where complicated paradigms are extracted to manage this problematic

task. Utilizing the primary data collected in this work, 2 DL-related CV methods are evaluated for automatic classification and detection of oral lesion for initial identification of oral cancers, these are image classifiers with object recognition with Faster R-CNN and ResNet-101. Huang et al. [17] introduced an intellectual multisampling tensor method for gaining cyst classification from MRI. To be Specific, this method initially encrypts the input image by 4 simple sampling functions, which allow the model to learn influential, and correlative features more regional, and global, and then the representation fusion method was implemented to merge those representations which are extracted. Then, those are contracted by a series of matrix product states, which mapped the input representation into high dimensional space for conducting a classifier operation.

3. The Proposed Model

In this article, a novel EJOADL-OCC system is formulated for automated oral cancer classification. The presented EJOADL-OCC system objectives for detecting and classifying the existence of oral cancer accurately and effectively. For accomplishing this, the introduced EJOADL-OCC technique follows MF-based noise elimination, ResNetv2 feature extractor, EJOA hyperparameter tuning, and CRBM-DBN classification. Fig. 1 portrays the process of the EJOADL-OCC method.

A. Stage I: Noise Removal

The presented EJOADL-OCC technique initially exploited the MF for the noise removal process. During the image processing, an MF was employed for removing noise in an image by exchanging the value of all the pixels with a median value of pixels from the local neighborhood nearby the pixels [18]. It is an effect of smoothing out the image and decreasing the count of noises present in the image. MFs can effectual at eliminating impulsive noise like salt-and-pepper noise that is caused by errors in image acquisition or broadcast. MFs can be comparatively easy for implementing and are executed to either grayscale or color images. It is also computationally effectual, making them a popular choice for image denoising.

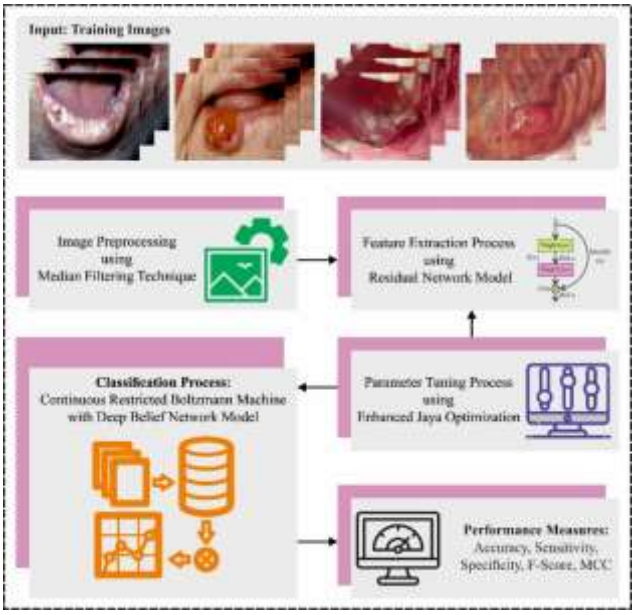

Figure 1: Complete process of the EJOADL-OCC model

B. Stage II: Feature Extraction

In this section, the feature vector generation procedure is achieved by the ResNetv2 model. With the prior deep network models, like Inception which attains effective outcomes when the networks go deep, it experiences a degradation in accuracy and rapid saturation. To resolve these issues, the idea of a Residual block was proposed [19]. The major idea is to present a shortcut bridge for slipping more than one layer. The conception is that, when the identity-mapping (x) is optimum, after the residual ($F(x)$) is disregarded by making them 0, viz., input = output. The concept of residual block works well and the ResNet50 architecture encompasses 5 stages, wherein in each phase, a group of residual and convolution blocks is presented. The ResNet101 is another variant of the ResNet paradigm. ResNet101 exactly follows a similar structure as ResNet50. In ResNet50 has six repetitive blocks of convolutional layers (all the blocks have 1x1,3x3,1x1 convolutional layers), while in ResNet101, the repetitive blocks are improved to 23.

ResNetV2 is an upgraded version of the ResNet family that accomplishes improved performance than ResNetVl. The underlying concept in the V2 architecture is on presenting a shortcut path to pass the data among the entire network and the residual block as follows:

$$y_1 = f(x_1, w_1) + h(x_1), x2 = f(y1) \tag{1}$$

Where, $x_1, x_2, .. i$ denotes the i^{th} residual units, $w_1, w_2, \ldots, i$ indicates the weighted of the specific residual unit, and f represents the residual function. Where $x_2 \equiv y_1$, then

$$x_2 = x_1 + f(x_1, w_1) \tag{2}$$

$$x_3 = x_2 + f(x_2, w_2) = x_1 + f(x_1, w_1) + f(x_2, w_2) \tag{3}$$

$$x_4 = x_3 + f(x_3, w_3) = x_1 + f(x_1, w_1) + f(x_2, w_2) + f(x_3, w_3) \tag{4}$$

$$x_i = x_1 + \sum_{k=1^{i-1}} f(x_k, w_k) \tag{5}$$

Eq. (5) affect the $bacl <$ propagation as follows.

$$\frac{\partial \phi}{\partial x_1} = \frac{\partial \phi}{\partial x_i} \cdot \frac{\partial x_i}{\partial x_1} = \frac{\partial \phi}{\partial x_i}\left(1 + \frac{\partial}{\partial x_1} \sum_{k=1^{i-1}} f(x_k, w_k)\right) \tag{6}$$

From the expression, ϕ denotes the loss function. Eqs. (5)-(6) determines that the signals can be easily communicated among each unit in forward and backward directions.

The EJOA is used to adjust the hyperparameters correlated to the ResNetv2 framework. In the study, a new presentation dependent upon 6 procedural stages is introduced for JOA [20]. Those steps might assist the researcher works on the optimization algorithm to easily apply these algorithms. Moreover, Algorithm1 illustrates the pseudocode of JOA. A detailed discussion of JOA steps is given below:

Step 1: Initialize the parameter of the optimization problem and JOA. Firstly the parameter of JOA is fixed. Remarkably, there is no control parameter in JOA. There only exist two algorithmic parameters namely *T* iteration numbers and *N* population size in the JOA. The constrained problems are normally modelled in the optimization context as in the following:

$$\min f(x) S.t. \begin{matrix} g_j(x) = c_j \ \forall j = (1,2, \ldots, n) \\ h_k(x) \le d_k \ \forall k = (1,2, \ldots, m) \end{matrix} \tag{7}$$

where $f(x)$ indicates the objective function which calculates the fitness values of the solution $x = (x_1, x_2, \ldots, x_D)$ in which x_i indicates the decision parameter allocated by the value in lower and upper bounds as $x_i \in [X_i^{\min}, X_i^{\max}]$. g_j denotes the j^{th} equality constraint and h_k is the k^{th} inequality constraint.

Step 2: Construction of the initial population. The first population (solution) of JOA is constructed and retained in the JAYA Memory (JM). It should be noted that JM is an amplified matrix of sizes $N \times D$ as demonstrated in Eq. (8) whereas N indicates the count of solutions and D represents the solution dimensional. Usually, the solution has been generated at random: $M_{ij} = X_j^{\min} + \left(X_j^{\min} - X_j^{\max}\right) \times rnd, \forall i \in (1, 2, \ldots, N) \wedge \forall j \in (1,2, \ldots, D)$. rnd shows the uniformly generated integer within [0,1].

$$JM = \begin{bmatrix} x_1^1 & x_2^1 & \ldots & x_D^1 \\ x_1^2 & x_2^2 & \ldots & x_D^2 \\ \vdots & \vdots & \ldots & \vdots \\ x_1^N & x_2^N & \ldots & x_D^N \end{bmatrix} \begin{bmatrix} f(x^1) \\ f(x^2) \\ \vdots \\ f(x^N) \end{bmatrix} \tag{8}$$

According to the objective function $f(x^i)$, all the solutions are evaluated and the JM solution is sorted in ascending order. Consequently, the better solution represents x^1 whereas the worst solution refers to x^N.

Step 3: JAYA Evolution procedure. Iteration by iteration, the decision variable of each solution in the JM endures variations utilizing the JAYA operator expressed in Eq. (9).

$$x_j'^i = x_j^i + r_1 \times \left(x_j^1 - \left|x_j^i\right|\right) - r_2 \times \left(x_j^N - \left|x_j^i\right|\right) \tag{9}$$

In Eq. (9), $x_j'^i$ indicates the newly upgraded solution; x_j^i denotes the existing solution. $x_j'^i$ represent the amended value of the decision value x_j^i. r_1 and r_2 represent the uniform function that generates a random integer ranging from zero to one [0,1]. This random number is utilized to accomplish the accurate balance betwixt the exploration as well as exploitation stages. Where x_j^1 indicates the j^{th} decision variables in the better solution whereas x_j^N denotes the j^{th} decision variables from the worse solution. The distance betwixt the decision variable of solutions and the worst solution and the current one determines the diversity control of JOA. High distance means high exploration and closest distance means high exploitation.

Step 4: Upgrade JM. The JM solution at all the iterations is upgraded. The objective function value of the newly generated solution $f(x'^i)$ is evaluated. The existing solution x^i is replaced with the new solution x'^i, where $f(x'^i) \leq f(x^i)$. This procedure is iterated as many as N.

Step 5: Stopping rule. Repeats step 3 and 4 until the ending condition of the maximal iteration amount T is attained.

A1gorithm 1: The pseudocode of JOA
Initialize the parameter of JOA and optimization problem (N, T, and so on.)
Randomly initialize a population of N solution.
Compute $f(X_i)\ \forall i = 1,2,\dots,N$
Sort the population: (x^1 and x^N denote the better and the worst solutions correspondingly).
$t = 1$
While ($t \leq T$) do
For $i = 1,\cdots,N$ do
For $j = 1,\cdots, D$ do
Set $r1 \in [0,1]$
Set $r_2 \in [0,1]$
$x_j^{'i} = x_j^i + r_1 \times (x_j^1 - \lvert x_j^i \rvert) - r_2 \times (x_j^N - \lvert x_j^i \rvert)$
End for
If $f(x'^i) \leq f(x^i)$ then
$x^i = x'^i$ {Update procedure}
End if
End for
$t = t + 1$
End while

Here, the EJOA is derived by employing logistic chaotic map. The chaotic map develops a robust approach for improving the efficacy of the Meta-heuristic system with the improvement of their arbitrariness variables [21]. This random parameter was removed based on uniform/Gaussian distribution; therefore it is accomplished optimum utilizing chaotic maps that share the same characteristic with superior performance. Managing this parameter by chaotic map reduces the local better and increases the convergence. Based on the outcome better chaotic map for this optimization is the logistic map. The general equation for the logistic chaotic map is:

$$\omega(\mathrm{t}+1) = a\omega(\mathrm{t})[1-\omega(t)], \qquad a = 4 \tag{10}$$

In which, $\omega(t)$ represents the value of chaotic maps at the t^{th} iteration. The primary condition of the chaotic maps can be regarded that 0.7 ($\omega(0) = 0.7$).

Fitness selection has a vital feature in the EJOA technique. A solution encoder could be employed to assess the goodness (aptitude) of candidate solutions. Here, the accuracy output is the fundamental conditions employed for designing a FF.

$$Fitness = \max(P) \tag{11}$$

$$P = \frac{TP}{TP + FP} \tag{12}$$

Whereas FP and TP designates the false and true positive values.

C. Stage III: Image Classification

Finally, the CRBM-DBN method has utilized for oral classification. As Hinton et al. introduced a novel trained model for DNN, the DBN is widely employed [22]. The DBN is stacked through a collection of RBMs that can comprehend a highly difficult relationships between hidden and visible units. Moreover, the unsupervised DBN and supervised regression system are combined to form semi-supervised framework that has improved representation capability. The architecture of RBM comprises a 2-layers: the input layer comprising visible unit $v = \{v_1, v_2, \dots, v_i\}$ and hidden layer comprising hidden unit $h = \{h_1, h_2, \dots, h_j\}$ and it is given as follows

$$E(v,h) = -\sum_{i=1}^{\nabla}\sum_{j=1}^{H} w_{ij}\, v_i h_j - \sum_{i=1}^{v} a_i\, v_i - \sum_{j=1}^{H} b_j\, h_j \tag{13}$$

Where v_i and h_j signify the state of i^{th} and j^{th} visible and hidden units, w_{ij} indicates the weight function, and a_j and b_j denote the bias function.

The trained procedure of DBN was recognized in 2 stages: pretraining, and finetuning. The contrast divergence (CD) technique adopts the weight parameter, and the backpropagation (BP) technique is exploited for finetuning the DBN. Fig. 2 portrays the DBN architecture.

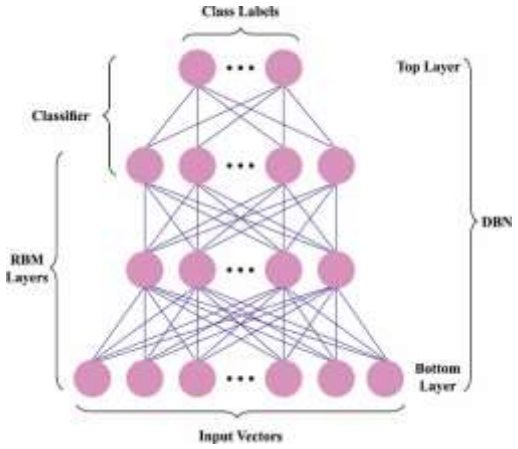

Figure 2: Architecture of DBN

Generally, traditional DBN architecture, the Softmax or LR has widely employed as the previous layers of the model, thereby the DBN could be well-adapted for resolving classifier problems. But the DBN is hardly utilized for regression problems. The typical classification of the DBN is enhanced by replacing RBM with CRBM, and the CRBM-DBN for classification is established. In CRBM, binary units in RBM can be exchanged with continuous stochastic unit, and the learning rules are "Minimalizing Contrastive Divergence" (MCD):

$$s_j = \varphi_j\left(\sum_i w_{ij}\, s_i + \sigma N_j(0,1)\right) \tag{14}$$

With

$$\phi_j(x_j) = \theta_L + \frac{(\theta_H - \theta_L)}{1 + e^{(-\alpha_j x_j)}} \tag{15}$$

Where s_i and s_j represent the conditions of the unit, j, $N_j(0,1)$ signifies a unit Gaussian, and σ denotes a constant. $\phi_j(x)$ indicates the sigmoid function, θ_H and θ_L represent the upper and lower asymptotes, and α defines the slope. The proposed method eliminates the Softmax or Logistic layer and employs the MSE of predictor for measuring the finetuning stage. Furthermore, the learning step is similar to DBN.

4. Results and Discussion

In this study, the analysis of the EJOADL-OCC approach is examined employing the oral cancer classification dataset from the Kaggle dataset [23], which has 131 images as depicted in Table 1. Fig. 3 depicts the instance imaging.

Figure 3: Sample images (a) Cancerous (b) Non-Cancerous

Table 1: Dataset specification

Class	Instance Numbers
Cancer	87
Non-Cancer	44
Overall Instances	131

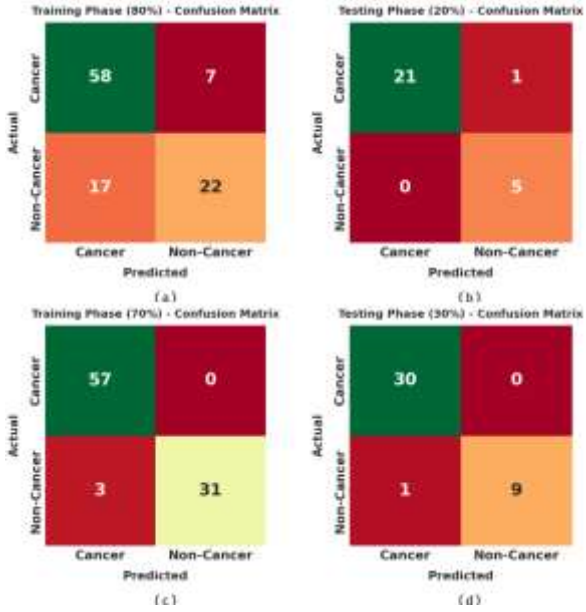

Figure 4: Confusion matrices of EJOADL-OCC method (a-b) 80:20 and (c-d) 70:30 TRP/TSP

The oral cancer classifier output of the EJOADL-OCC methodology are investigated by the confusion matrix in Fig. 4. The simulated validation portrayed that the EJOADL-OCC methodology could be proficiently identified cancer and non-cancer images.

In Table 2, a brief oral cancer classifier outputs of the EJOADL-OCC technique with 80:20 of TRS/TSS is offered. Fig. 5 examines the overall outputs of the EJOADL-OCC method with 80% of TRS. The outputs ensured that the EJOADL-OCC method identified cancer and non-cancer samples. For instance, under cancer class, the EJOADL-OCC method obtains $accu_{bal}$ of 72.82%, $sens_y$ of 72.82%, $spec_y$ of 72.82%, F_{score} of 73.78%, and MCC of 49.27%. Eventually, under the non-cancer class, the EJOADL-OCC system acquires $accu_{bal}$ of 56.41%, $sens_y$ of 56.41%, $spec_y$ of 89.23%, F_{score} of 64.71%, and MCC of 49.27%.

Table 2: Oral cancer classifier output of EJOADL-OCC method on 80:20 of TRS/TSS

Class	$Accu_{bal}$	$Sens_y$	$Spec_y$	F_{score}	MCC
TRS (80%)					
Cancer	89.23	89.23	56.41	82.86	49.27
Non-Cancer	56.41	56.41	89.23	64.71	49.27
Average	72.82	72.82	72.82	73.78	49.27
TSS (20%)					
Cancer	95.45	95.45	100.00	97.67	89.19
Non-Cancer	100.00	100.00	95.45	90.91	89.19
Average	97.73	97.73	97.73	94.29	89.19

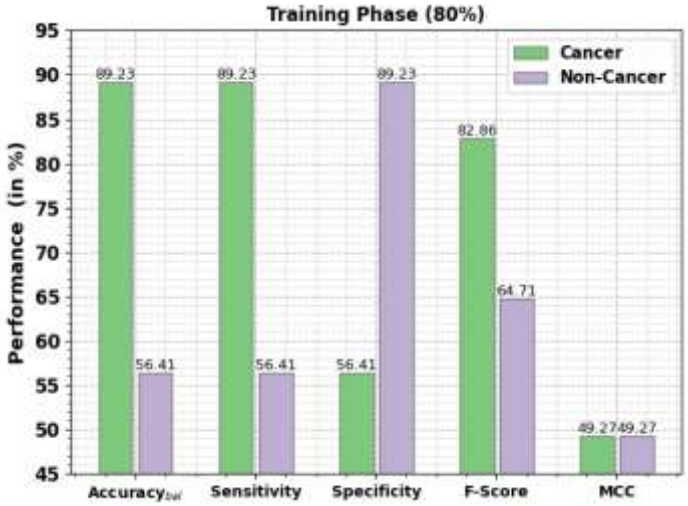

Figure 5: Oral cancer classifier outcome of EJOADL-OCC method on 80% of TRS

Fig. 6 exhibits the overall outputs of the EJOADL-OCC algorithm with 20% of TSS. The outputs make sure that the EJOADL-OCC method detected cancer and non-cancer samples. For instance, under cancer class, the EJOADL-OCC method gains $accu_{bal}$ of 95.45%, $sens_y$ of 95.45%, $spec_y$ of 100%, F_{score} of 97.67%, and MCC of 89.19%. Finally, under the non-cancer class, the EJOADL-OCC approach achieves $accu_{bal}$ of 100%, $sens_y$ of 100%, $spec_y$ of 95.45%, F_{score} of 90.91%, and MCC of 89.19%.

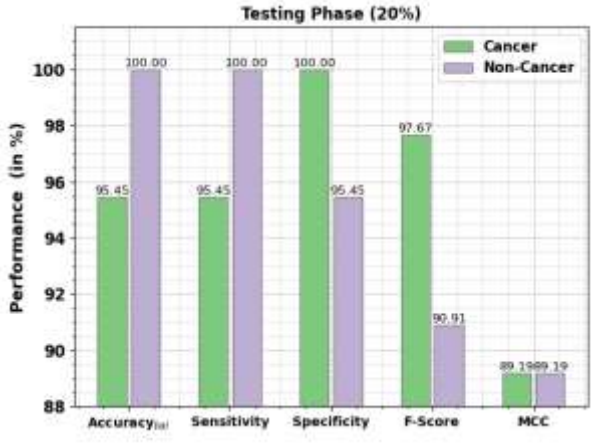

Figure 6: Oral cancer classifier output of EJOADL-OCC method on 20% of TSS

In Table 3, a detailed oral cancer classifier result of the EJOADL-OCC methodology with 70:30 of TRS/TSS is offered. Fig. 7 inspects the overall outcome of the EJOADL-OCC method with 70% of TRS. The results make sure that the EJOADL-OCC system identified cancer and non-cancer samples. For example, under cancer class, the EJOADL-OCC algorithm gains $accu_{bal}$ of 100%, $sens_y$ of 100%, $spec_y$ of 91.18%, F_{score} of 97.44%, and MCC of 93.07%. Furthermore, under the non-cancer class, the EJOADL-OCC method reaches an $accu_{bal}$ of 91.18%, $sens_y$ of 91.18%, $spec_y$ of 100%, F_{score} of 95.38%, and MCC of 93.07%.

Table 3: Oral cancer classifier output of EJOADL-OCC method on 70:30 of TRS/TSS

Class	$Accu_{bal}$	$Sens_y$	$Spec_y$	F_{score}	MCC
Training Phase (70%)					
Cancer	100.00	100.00	91.18	97.44	93.07
Non-Cancer	91.18	91.18	100.00	95.38	93.07
Average	95.59	95.59	95.59	96.41	93.07
Testing Phase (30%)					
Cancer	100.00	100.00	90.00	98.36	93.33
Non-Cancer	90.00	90.00	100.00	94.74	93.33
Average	95.00	95.00	95.00	96.55	93.33

Figure 7: Oral cancer classifier outcome of EJOADL-OCC method on 70% of TRS

Fig. 8 exhibits the overall experimental outputs of the EJOADL-OCC methodology with 30% of TSS. The experimental data referred that the EJOADL-OCC methodology that identified cancer and non-cancer samples. For instance, under cancer class, the EJOADL-OCC technique attains $accu_{bal}$ of 100%, $sens_y$ of 100%, $spec_y$ of 90%, F_{score} of 98.36%, and MCC of 93.33%. At last, under the non-cancer class, the EJOADL-OCC technique obtains $accu_{bal}$ of 90%, $sens_y$ of 90%, $spec_y$ of 100%, F_{score} of 94.74%, and MCC of 93.33%.

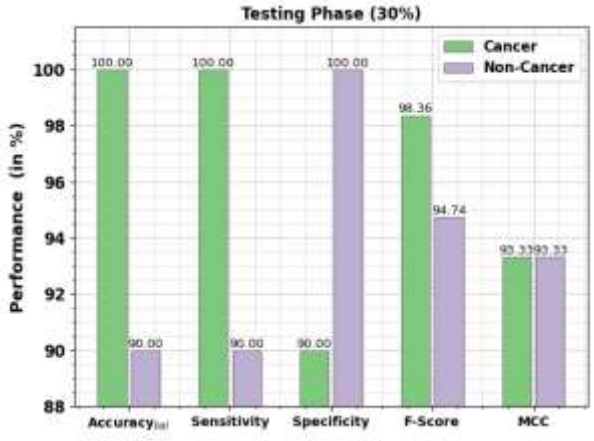

Figure 8: Oral cancer classifier outcome of EJOADL-OCC approach on 30% of TSS

The TACY and VACY of the EJOADL-OCC method are inspected on oral cancer achievement in Fig. 9. The figure demonstrated that the EJOADL-OCC methodology has exhibited better outcome with highest values. The EJOADL-OCC model has gained optimal TACY outcome.

The TLOS and VLOS of the EJOADL-OCC method are inspected on oral cancer achievement in Fig. 10. The figure indicated that the EJOADL-OCC algorithm has exhibited improved outcome with the smallest values. It can be evident that the EJOADL-OCC method has resulted in lesser VLOS outcome.

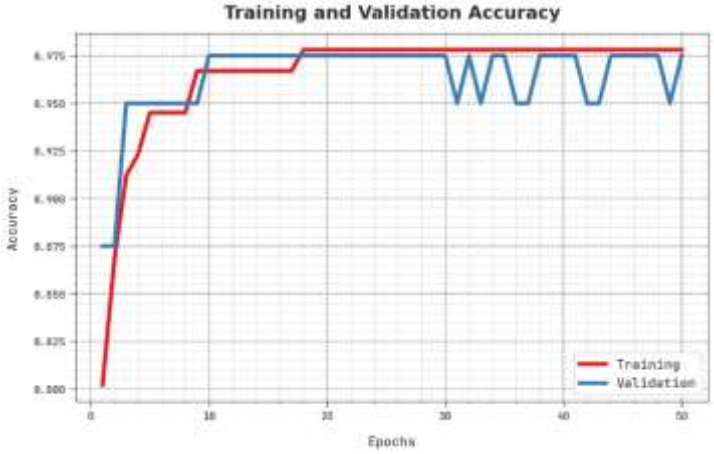

Figure 9: TACY and VACY curve of EJOADL-OCC method

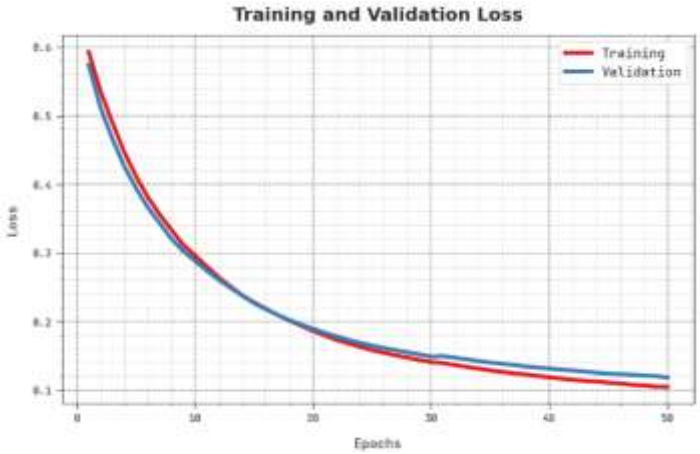

Figure 10: TLOS and VLOS curve of EJOADL-OCC method

An evident PR curve of the EJOADL-OCC technique in the test dataset is exposed in Fig. 11. The figure indicated that the EJOADL-OCC method has resulted in highest PR values under two classes.

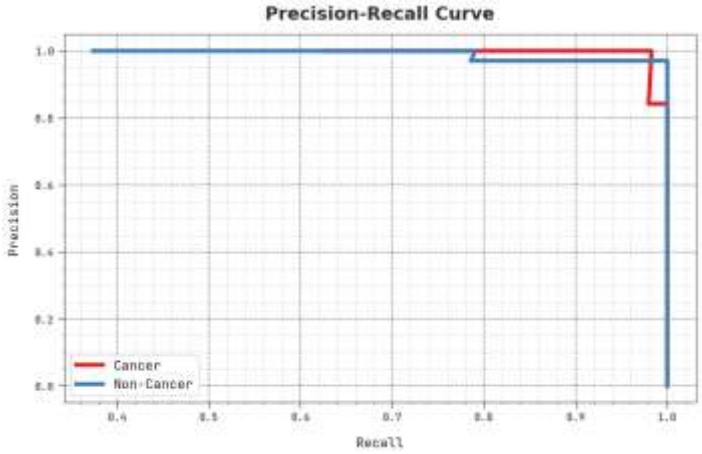

Figure 11: PR outcome of EJOADL-OCC method

An elaborated ROC study of the EJOADL-OCC methodology in the test dataset is shown in Fig. 12. The output stated the EJOADL-OCC approach has depicted its ability in categorizing two classes.

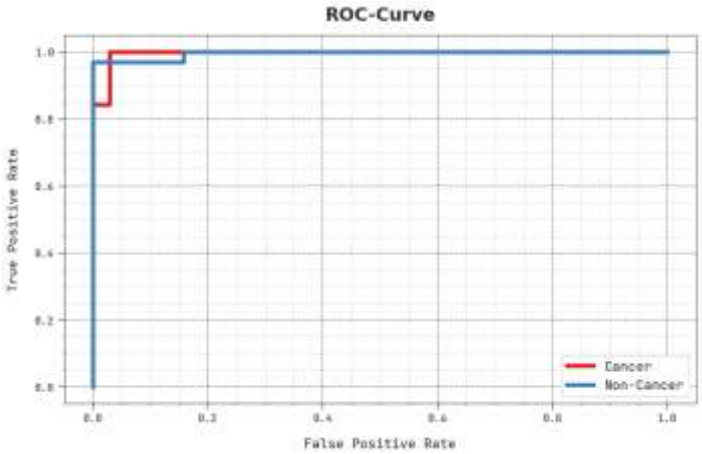

Figure 12: ROC curve of EJOADL-OCC method

In Table 4, a widespread relational study of the EJOADL-OCC with other DL methods is given [24]. In Fig. 13, a comparative $accu_y$ and F_{score} examination of the EJOADL-OCC method is provided. The outputs inferred that the EJOADL-OCC system attains maximum $accu_y$ and F_{score} values. Based on $accu_y$, the EJOADL-OCC system obtained an increasing $accu_y$ of 97.73% whereas the CNN, OID-CNN, DBN, Inception-v4, and DenseNet-161 models attain a reducing $accu_y$ of 93.78%, 97.35%, 86.51%, 85.26%, and 89.61% correspondingly.

Table 4: Relative outcome of EJOADL-OCC method with other DL approaches

Methods	$Accu_y$	$Sens_y$	$Spec_y$	F_{score}
EJOADL-OCC	97.73	97.73	97.73	94.29
CNN Model	93.78	94.38	96.91	92.34
OID-CNN Model	97.35	97.14	97.25	93.18
DBN Model	86.51	84.31	91.53	85.88
Inception-v4 Model	85.26	86.89	89.60	87.09
DenseNet-161 Model	89.61	88.19	85.69	86.49

Moreover, concerning F_{score}, the EJOADL-OCC method attained an improved F_{score} of 94.29% whereas the CNN, OID-CNN, DBN, Inception-v4, and DenseNet-161 methods reach lesser F_{score} of 92.34%, 93.18%, 85.88%, 87.09%, and 86.49% correspondingly.

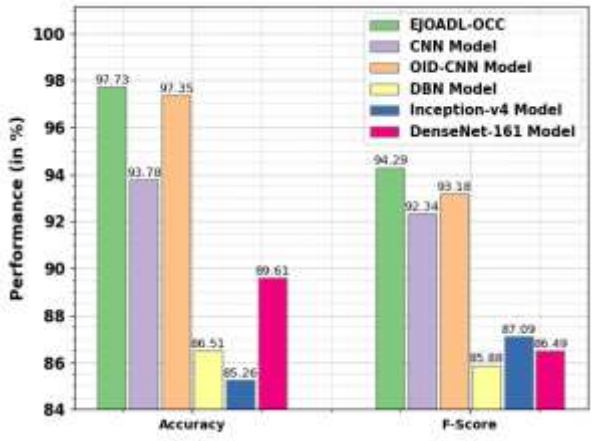

Figure 13: $Accu_y$ and F_{score} analysis of EJOADL-OCC method with other DL techniques

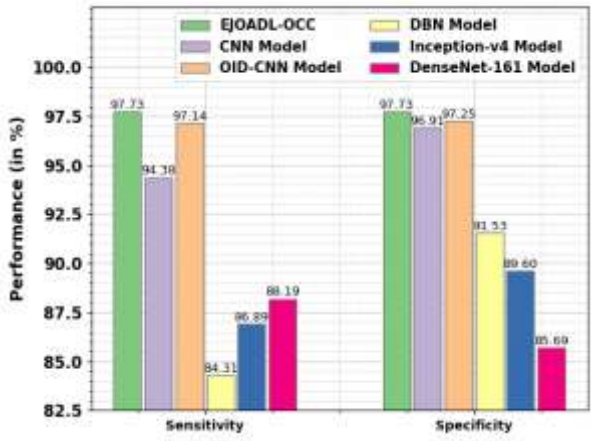

Figure 14: $Sens_y$ and $spec_y$ analysis of EJOADL-OCC technique with other DL methods

In Fig. 14, a relative $sens_y$ and $spec_y$ study of the EJOADL-OCC approach is provided. The outcomes stated that the EJOADL-OCC approach achieves maximal values of $sens_y$ and $spec_y$. Concerning $sens_y$, the EJOADL-OCC system obtained an increasing $sens_y$ of 97.73% whereas the CNN, OID-CNN, DBN, Inception-v4, and DenseNet-161 systems attain lower $sens_y$ of 94.38%, 97.14%, 84.31%, 86.89%, and 88.19% correspondingly. Additionally, based on $spec_y$, the EJOADL-OCC system acquired a maximal $spec_y$ of 97.73% whereas the CNN, OID-CNN, DBN, Inception-v4, and DenseNet-161 algorithms gain decreased $spec_y$ of 96.91%, 97.25%, 91.53%, 89.60%, and 85.69% correspondingly.

These outputs stated the maximum achievement of the EJOADL-OCC approach on classifying oral cancer.

5. Conclusion

In this study, a novel EJOADL-OCC approach was developed for automated oral cancer classification. The objective of the proposed EJOADL-OCC approach is to precisely detect and categorize the oral cancer presence. For this, the presented EJOADL-OCC approach initially exploits MF for noise elimination. Next, the feature vector generation process is performed by the ResNetv2 model with EJOA as a hyperparameter optimizer. For accurate classification of oral cancer, the CRBM-DBN model is utilized. The investigational evaluation of the EJOADL-OCC method was experimented by implementing a series of analysis and the experimental outputs demonstrate its supremacy over other DL algorithm. Thus, the EJOADL-OCC method can be employed for precisely identifying the oral cancer. In the future, the classification outcome of the EJOADL-OCC method can be boosted by hybrid DL feature extractors.

Funding: "This research received no external funding"

Conflicts of Interest: "The authors declare no conflict of interest."

References

[1] Lin, H., Chen, H., Weng, L., Shao, J. and Lin, J., 2021. Automatic detection of oral cancer in smartphone-based images using deep learning for early diagnosis. Journal of Biomedical Optics, 26(8), p.086007.

[2] López-Cortés, X.A., Matamala, F., Venegas, B. and Rivera, C., 2022. Machine-Learning Applications in Oral Cancer: A Systematic Review. Applied Sciences, 12(11), p.5715.

[3] Prabhakaran, R. and Mohana, D.J., 2020. Detection of Oral Cancer Using Machine Learning Classification Methods. International Journal of Electrical Engineering and Technology, 11(3).

[4] Sharma, D., Kudva, V., Patil, V., Kudva, A. and Bhat, R.S., 2022. A Convolutional Neural Network Based Deep Learning Algorithm for Identification of Oral Precancerous and Cancerous Lesion and Differentiation from Normal Mucosa: A Retrospective Study. Engineered Science, 18, pp.278-287.

[5] Kouznetsova, V.L., Li, J., Romm, E. and Tsigelny, I.F., 2021. Finding distinctions between oral cancer and periodontitis using saliva metabolites and machine learning. Oral diseases, 27(3), pp.484-493.

[6] Siddalingappa, R. and Kanagaraj, S., 2022. K-nearest-neighbour algorithm to predict the survival time and classification of various stages of oral cancer: a machine learning approach. F1000Research, 11(70), p.70.

[7] Fu, Q., Chen, Y., Li, Z., Jing, Q., Hu, C., Liu, H., Bao, J., Hong, Y., Shi, T., Li, K. and Zou, H., 2020. A deep learning algorithm for detection of oral cavity squamous cell carcinoma from photographic images: A retrospective study. EClinicalMedicine, 27, p.100558.

[8] Bansal, K., Batla, R.K., Kumar, Y. and Shafi, J., 2022. Artificial Intelligence Techniques in Health Informatics for Oral Cancer Detection. In Connected e-Health (pp. 255-279). Springer, Cham.

[9] Song, B., Li, S., Sunny, S., Gurushanth, K., Mendonca, P., Mukhia, N., Patrick, S., Gurudath, S., Raghavan, S., Tsusennaro, I. and Leivon, S.T., 2021. Classification of imbalanced oral cancer image data from high-risk population. Journal of biomedical optics, 26(10), p.105001.

[10] Rauf, A.R.A., Isa, W.H.M., Khairuddin, I.M., Razman, M.A.M., Arzmi, B.M.H. and Majeed, A.P.A., 2022. The Classification of Oral Squamous Cell Carcinoma (OSCC) by Means of Transfer Learning. In Robot Intelligence Technology and Applications 6: Results from the 9th International Conference on Robot Intelligence Technology and Applications (Vol. 429, p. 386). Springer Nature.

[11] Lim, J.H., Tan, C.S., Chan, C.S., Welikala, R.A., Remagnino, P., Rajendran, S., Kallarakkal, T.G., Zain, R.B., Jayasinghe, R.D., Rimal, J. and Kerr, A.R., 2021, July. D'OraCa: deep learning-based classification of oral lesions with mouth landmark guidance for early detection of oral cancer. In Annual Conference on Medical Image Understanding and Analysis (pp. 408-422). Springer, Cham.

[12] Tanriver, G., Soluk Tekkesin, M. and Ergen, O., 2021. Automated detection and classification of oral lesions using deep learning to detect oral potentially malignant disorders. Cancers, 13(11), p.2766.

[13] Lu, J., Sladoje, N., Runow Stark, C., Darai Ramqvist, E., Hirsch, J.M. and Lindblad, J., 2020, June. A deep learning based pipeline for efficient oral cancer screening on whole slide images. In International Conference on Image Analysis and Recognition (pp. 249-261). Springer, Cham.

[14] Jeyaraj, P.R. and Samuel Nadar, E.R., 2019. Computer-assisted medical image classification for early diagnosis of oral cancer employing deep learning algorithm. Journal of cancer research and clinical oncology, 145(4), pp.829-837.

[15] Shamim, M.Z.M., Syed, S., Shiblee, M., Usman, M., Ali, S.J., Hussein, H.S. and Farrag, M., 2022. Automated detection of oral pre-cancerous tongue lesions using deep learning for early diagnosis of oral cavity cancer. The Computer Journal, 65(1), pp.91-104.

[16] Welikala, R.A., Remagnino, P., Lim, J.H., Chan, C.S., Rajendran, S., Kallarakkal, T.G., Zain, R.B., Jayasinghe, R.D., Rimal, J., Kerr, A.R. and Amtha, R., 2020. Automated detection and classification of oral lesions using deep learning for early detection of oral cancer. IEEE Access, 8, pp.132677-132693.

[17] Huang, C., Zhang, G., Chen, S. and de Albuquerque, V.H.C., 2022. An Intelligent Multisampling Tensor Model for Oral Cancer Classification. IEEE Transactions on Industrial Informatics, 18(11), pp.7853-7861.

[18] Ahmed Abdelhafeez, Hoda K. Mohamed, Skin Cancer Detection using Neutrosophic c-means and Fuzzy c-means Clustering Algorithms, Journal of Intelligent Systems and Internet of Things, Vol. 8 , No. 1 , (2023) : 33-42 (Doi : https://doi.org/10.54216/JISIoT.080103).

[19] Eman Shawky Mira,Ahmed M. Saaduddin Sapri,Rowaa F. Aljehanı,Bayan S. Jambı,Taseer Bashir,El-Sayed M. El-Kenawy,Mohamed Saber, Early Diagnosis of Oral Cancer Using Image Processing and Artificial

Intelligence, Fusion: Practice and Applications, Vol. 14 , No. 1 , (2024) : 293-308 (Doi : https://doi.org/10.54216/FPA.140122).

[20] Zitar, R.A., Al-Betar, M.A., Awadallah, M.A., Doush, I.A. and Assaleh, K., 2022. An intensive and comprehensive overview of JOA, its versions and applications. Archives of Computational Methods in Engineering, 29(2), pp.763-792.

[21] Parthiban, S., Harshavardhan, A., Neelakandan, S., Prashanthi, V., Alhassan Alolo, A.R.A. and Velmurugan, S., 2022. Chaotic Salp Swarm Optimization-Based Energy-Aware VMP Technique for Cloud Data Centers. Computational Intelligence and Neuroscience, 2022.

[22] Zhao, X., Liu, D. and Yan, X., 2023. Diameter Prediction of Silicon Ingots in the Czochralski Process Based on a Hybrid Deep Learning Model. Crystals, 13(1), p.36.

[23] https://www.kaggle.com/datasets/shivam17299/oral-cancer-lips-and-tongue-images

[24] Alabdan, R.; Alruban, A.; Hilal, A.M.; Motwakel, A. Artificial-Intelligence-Based Decision Making for Oral Potentially Malignant Disorder Diagnosis in Internet of Medical Things Environment. Healthcare 2023, 11, 113. https://doi.org/10.3390/healthcare 11010113